Microstructural analysis of 9.7% efficient Cu2ZnSnSe4 thin film solar cells

M. Buffière, G. Brammertz, M. Batuk, C. Verbist, D. Mangin, C. Koble, J. Hadermann, M. Meuris, and J. Poortmans

Citation: Applied Physics Letters **105**, 183903 (2014); doi: 10.1063/1.4901401
View online: http://dx.doi.org/10.1063/1.4901401
View Table of Contents: http://scitation.aip.org/content/aip/journal/apl/105/18?ver=pdfcov
Published by the AIP Publishing

Articles you may be interested in

The impact of oxygen incorporation during intrinsic ZnO sputtering on the performance of Cu(In,Ga)Se2 thin film solar cells
Appl. Phys. Lett. **105**, 083906 (2014); 10.1063/1.4894214

Intermixing at the absorber-buffer layer interface in thin-film solar cells: The electronic effects of point defects in Cu(In,Ga)(Se,S)2 and Cu2ZnSn(Se,S)4 devices
J. Appl. Phys. **116**, 063505 (2014); 10.1063/1.4892407

Characterization of defects in 9.7% efficient Cu2ZnSnSe4-CdS-ZnO solar cells
Appl. Phys. Lett. **103**, 163904 (2013); 10.1063/1.4826448

Control of an interfacial MoSe2 layer in Cu2ZnSnSe4 thin film solar cells: 8.9% power conversion efficiency with a TiN diffusion barrier
Appl. Phys. Lett. **101**, 053903 (2012); 10.1063/1.4740276

High efficiency thin-film Cu In 1 − x Ga x Se 2 photovoltaic cells using a Cd 1 − x Zn x S buffer layer
Appl. Phys. Lett. **89**, 253503 (2006); 10.1063/1.2410230

This article is copyrighted as indicated in the article. Reuse of AIP content is subject to the terms at: http://scitation.aip.org/termsconditions. Downloaded to IP: 143.129.150.67 On: Fri, 07 Nov 2014 16:31:50

Microstructural analysis of 9.7% efficient $Cu_2ZnSnSe_4$ thin film solar cells

M. Buffière,[1,2,a)] G. Brammertz,[3,4] M. Batuk,[5] C. Verbist,[5] D. Mangin,[6] C. Koble,[7] J. Hadermann,[5] M. Meuris,[3,4] and J. Poortmans[1,2,4]
[1]*Department of Electrical Engineering (ESAT), KU Leuven, Kasteelpark Arenberg 10, 3001 Heverlee, Belgium*
[2]*imec—partner in Solliance, Kapeldreef 75, 3001 Leuven, Belgium*
[3]*imec division IMOMEC—partner in Solliance, Wetenschapspark 1, 3590 Diepenbeek, Belgium*
[4]*Institute for Material Research (IMO), Hasselt University, Wetenschapspark 1, 3590 Diepenbeek, Belgium*
[5]*Electron Microscopy for Materials Science (EMAT), University of Antwerp, Groenenborgerlaan 171, 2020 Antwerp, Belgium*
[6]*Institut Jean Lamour, Université de Lorraine, Parc de Saurupt, CS 50840, 54011 Nancy cedex, France*
[7]*Helmholtz-Zentrum Berlin für Materialien und Energie GmbH, Hahn-Meitner-Platz 1, 14109 Berlin, Germany*

(Received 17 August 2014; accepted 28 October 2014; published online 7 November 2014)

This work presents a detailed analysis of the microstructure and the composition of our record $Cu_2ZnSnSe_4$ (CZTSe)-CdS-ZnO solar cell with a total area efficiency of 9.7%. The average composition of the CZTSe crystallites is $Cu_{1.94}Zn_{1.12}Sn_{0.95}Se_{3.99}$. Large crystals of ZnSe secondary phase (up to 400 nm diameter) are observed at the voids between the absorber and the back contact, while smaller ZnSe domains are segregated at the grain boundaries and close to the surface of the CZTSe grains. An underlying layer and some particles of Cu_xSe are observed at the Mo-$MoSe_2$-$Cu_2ZnSnSe_4$ interface. The free surface of the voids at the back interface is covered by an amorphous layer containing Cu, S, O, and C, while the presence of Cd, Na, and K is also observed in this region. © *2014 AIP Publishing LLC*. [http://dx.doi.org/10.1063/1.4901401]

The $Cu_2ZnSn(S,Se)_4$ (CZTSSe) compounds are being extensively studied as a possible absorber material for solar cells in order to offer cheap and reliable alternatives to $Cu(In,Ga)(S,Se)_2$ (CIGSSe) or CdTe photovoltaic thin film technologies.[1–4] The fundamental properties of these materials look very promising[5–7] since devices with an efficiency up to 12.6% have been already demonstrated.[7] However, the control of the composition and the microstructure in such materials is challenging, due to the limited stability of the kesterite compound. Various undesirable secondary phases,[8–12] such as Zn(S,Se), $Cu_x(S,Se)$, $Sn(S,Se)_x$, or $Cu_2Sn(S,Se)_3$, can be formed during the processing of the absorber layer and hinder the electrical performances of the solar cells. Furthermore, high density of voids is often observed at the back contact/absorber interface, which could come from the decomposition reaction of CZTSSe in contact with the Mo substrate.[13,14]

In previous work,[15] we have shown that, using $Cu_2ZnSnSe_4$ (CZTSe)/CdS heterojunction cells, we can prepare a $1 \times 1\,cm^2$ solar cell with 9.7% efficiency. In that case, the CZTSe absorber was grown by a two-step process consisting of DC-sputtering of $Cu_{10}Sn_{90}$ (230 nm), Zn (140 nm), and Cu (100 nm), followed by a thermal annealing in H_2Se atmosphere. The average composition of the as grown absorber layer was determined as [Cu]/([Zn]+[Sn]) = 0.7, [Zn]/[Sn] = 1.02 and [Se]/([Cu]+[Zn]+[Sn]) = 1.08, as measured from energy dispersive X-ray (EDX) spectroscopy (accelerating voltage of 20 kV, measured area of $50 \times 50\,\mu m^2$). For solar cell processing, a procedure developed for CIGSSe based solar cells was used, consisting of potassium cyanide etch, chemical bath deposition at 60 °C of a thin n-type CdS buffer layer, and AC-sputtering of 120 nm of intrinsic ZnO followed by 250 nm of highly Al-doped ZnO.[16,17] More details on the preparation of the samples can be found elsewhere.[15] In this contribution, we report on the detailed morphological and structural study of this solar cell using scanning and transmission electron microscopy (SEM, TEM) and secondary ions mass spectroscopy (SIMS) measurements. SEM analyses (*Nova*, FEI) were performed using an accelerating voltage of 5 kV. The specimen for TEM analysis was prepared by the focused ion beam (FIB) technique, on a Mo support. High angle annular dark field scanning transmission electron microscopy (HAADF-STEM) images and overview STEM-EDX maps were acquired using a FEI Titan 80–300 "cubed" microscope equipped with a Super-X detector and operated at 300 kV. EDX maps were generated from the intensity of the Cu-K, Zn-K, Sn-L, Se-K, Cd-L, S-K, O-K, C-K, and Mo-K lines. Note that the S-K and Mo-L lines overlap (2.31 and 2.29 keV, respectively). SIMS measurements (*Cameca IMS 7f* system) were performed using an impact energy of 3 keV and a 55 nA Cs^+ beam and detecting MCs^+ complexes with $M = {}^{63}Cu$, ${}^{66}Zn$, ${}^{120}Sn$, ${}^{78}Se$, ${}^{114}Cd$, ${}^{34}S$, ${}^{16}O$, and ${}^{98}Mo$, and also ${}^{23}Na^+$, ${}^{39}K^+$ species.

Figure 1 shows cross-section SEM images of the complete device. The thickness of the CZTSe layer is about 1 μm. Although the absorber appears to be relatively thin, the external quantum efficiency (EQE) measurement previously performed on this solar cell[15] does not show specific decrease of the charge collection in the long wavelength range, due to the very high absorption coefficient of CZTSe. Some additional features are visible in CZTSe absorber layer which are highlighted by yellow arrows: the presence of 50 nm to 400 nm large individual grains of secondary phases (in light grey on the SEM images) and of interconnected voids mainly located at the back contact/absorber interface (Fig. 1(a)); the inclusion of smaller domains of secondary

a)Electronic mail: buffiere@imec.be

 © 2014 AIP Publishing LLC

This article is copyrighted as indicated in the article. Reuse of AIP content is subject to the terms at: http://scitation.aip.org/termsconditions. Downloaded to IP: 143.129.150.67 On: Fri, 07 Nov 2014 16:31:50

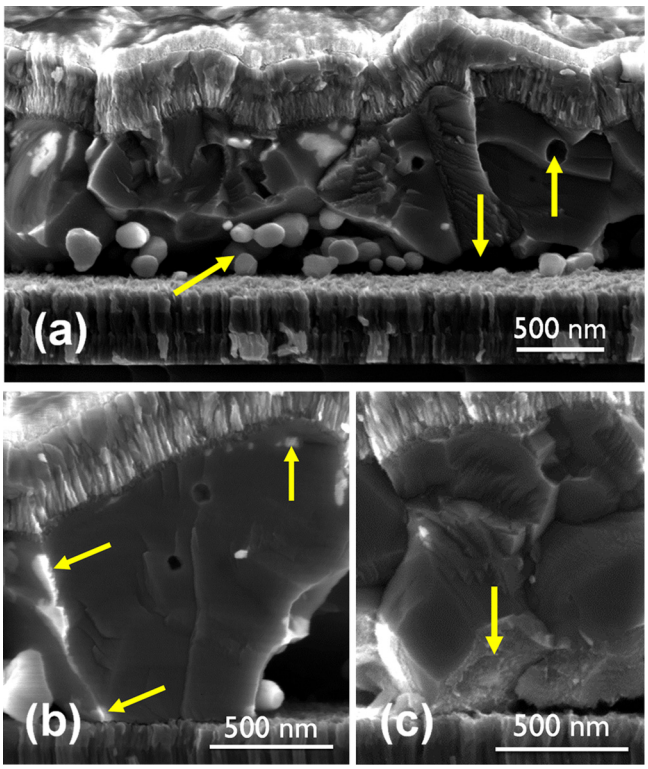

FIG. 1. Cross-section SEM images of the solar cell focused on the CZTSe absorber showing (a) the presence of voids and secondary phases at the bottom interface, (b) the segregation of secondary phases at the CZTSe grain boundaries and free surfaces and (c) some thin layer covering the free surface of the bottom CZTSe grains.

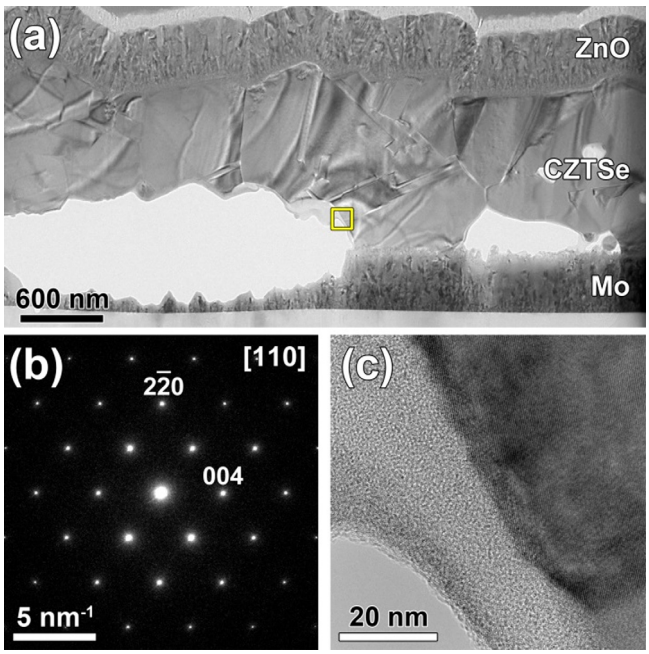

FIG. 2. (a) Overview TEM image of the Mo-CZTSe-CdS-ZnO solar cell; (b) ED pattern from one of the CZTSe grains; (c) HR TEM image of the area outlined with yellow square: the CZTSe grain is covered by a thin (~20 nm) amorphous layer.

phases within the absorber crystals, visible at the CZTSe grain boundaries and free surfaces (Fig. 1(b)). As this secondary phase appears brighter than the CZTSe grains on the SEM micrographs, it might be ZnSe crystals.[18] ZnSe is a low n-doped wide band gap material; therefore, its presence as isolated grains or domains within the absorber layer is believed not to hinder the electrical performance of the solar cells. Furthermore, a previous study has shown that grain boundary passivation can be achieved in CZTS via precipitation of certain secondary phases, such as ZnS.[19] We also observed the presence of a thin layer covering the free bottom surface of some CZTSe grains (Fig. 1(c)).

Figure 2(a) shows an overview TEM image of the CZTSe-CdS-ZnO solar cell. The sample is composed of large grains of CZTSe, with a width varying from 280 to 1000 nm. An example of the electron diffraction (ED) pattern taken from the large grain is given in Figure 2(b). The pattern can be indexed using the data for tetragonal $Cu_2ZnSnSe_4$ (#52–868, I-42 m space group, a = 5.693(1) Å, c = 11.333(1) Å). As already observed on Figure 1(a), one particularity of our samples becomes apparent in the cross section TEM image, namely, the large amount of holes on the backside of the sample (note that the large hole is from the sample thinning). The origin of the holes could either be due to the unstable nature of CZTSe in contact with Mo, as reported in Ref. 14, or it could arise because we use the low melting point $Cu_{10}Sn_{90}$ metal layer as the first layer in contact with the Mo. This layer could liquefy during the first stages of the selenization and does not present good wetting properties on Mo. It is obvious that these voids are not very helpful for good adhesion of the absorber layer on the Mo backside contact, as the absorber layer easily peels off the Mo backside upon mechanical stress. However, they could improve the backside contact passivation and, thereby, the charge collection, depending on the properties of the free surface of the CZTSe grains at this particular location. The high resolution TEM image acquired in this area—corresponding to the location of the yellow square in Figure 2(a)—is shown in Figure 2(c). We observe the segregation of amorphous matter on the edge of the CZTSe grain, with a thickness of ~20 nm.

To investigate the phase uniformity of the CZTSe absorber and the composition of this amorphous covering layer, HAADF-STEM images and overview STEM-EDX maps were acquired. The results are shown in Figure 3. EDX analysis and ED pattern[20] confirmed the presence of small (~50–100 nm) ZnSe inclusions close to the top and bottom surfaces of the CZTSe layer and at the grain boundaries. We also found one Cu and Se rich particle (with a size of ~80 nm) at the bottom of the CZTSe grain, which composition is close to Cu_2Se according to EDX. While this Cu_2Se particle was noticed only in one area (as marked in the mixed map in Figure 3 with the yellow arrow), ZnSe grains were more common (as indicated by blue arrows).[20] Furthermore, the amorphous 20–30 nm thick layer covering the free surface of the CZTSe crystals at the location of the voids contains mainly Cu, S, O, and some C-rich aggregates. The presence of Cu-rich and ZnSe phases at the absorber/back contact interface tends to confirm the decomposition of the kesterite phase into binary compounds at this location, although no Cu_xSnSe_y compound could be found. The liquefaction of CuSe at relatively low temperature could explain that this phase is forming a continuous layer while ZnSe is more segregating into clusters of various sizes. The presence of organic matter (C, O) and S in the amorphous layer could

This article is copyrighted as indicated in the article. Reuse of AIP content is subject to the terms at: http://scitation.aip.org/termsconditions. Downloaded to IP: 143.129.150.67 On: Fri, 07 Nov 2014 16:31:50

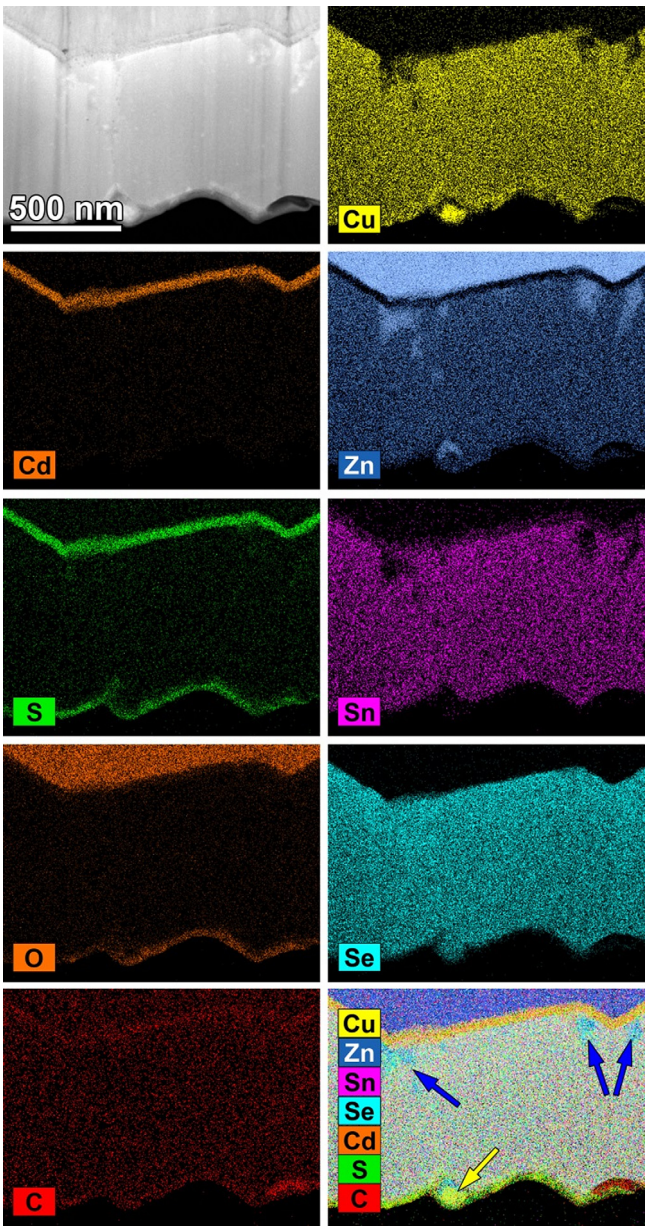

FIG. 3. EDX elemental maps taken from the CZTSe solar cell (elements detected: Cu, Zn, Sn, Se, Cd, S, O, and C) and a mixed map. Arrows point the inclusions of the secondary phases: yellow—to the Cu_2Se, blue—to the ZnSe.

come from the chemical bath solution used for the deposition of the CdS buffer layer, although no Cd could be found at this location. As this solar cell exhibits reasonable minority carrier lifetime ($\tau = 7$ ns) and large EQE values in the long wavelength range (>80% at 100 nm),[15] the presence of this amorphous layer is believed not to be detrimental for the efficiency of the device. For the rest, the grains are uniform. The composition of 15 CZTSe crystallites was measured. An average atomic ratio between Cu/Zn/Sn/Se was found to be 24.2(6):14.0(5):11.9(4):49.9(8), which gives the composition $Cu_{1.94(5)}Zn_{1.12(4)}Sn_{0.95(4)}Se_{3.99(7)}$. This composition [Cu]/([Zn]+[Sn]) = 0.9 and [Zn]/[Sn] = 1.2) is very close to other compositions reported in literature that yield best results.[6] Interestingly, it means that the particularly low doping observed in this device (of the order of 10^{15} cm^{-3}) does not seem to be due to a low Cu-content[10] or [Zn]/[Sn] ratio[21] within the kesterite phase.

To gain a detailed understanding of the interfaces in CZTSe solar cells, we performed high magnification TEM and composition profile analysis at both the front and back interfaces, as shown in Figure 4. The EDX profile from the CZTSe-CdS-ZnO region reveals that the CdS buffer layer also contains some O, which might come from $Cd(OH)_2$ compounds formed in the basic solution due to competitive chemical reactions:

$$Cd^{2+}{}_{(aq)} + S^{2-}{}_{(aq)} = CdS_{(s)}, \quad k_{s1} = 10^{-22.3},$$

$$Cd^{2+}{}_{(aq)} + 2OH^{-}{}_{(aq)} = Cd(OH)_{2(s)}, \quad k_{s2} = 10^{-12.5},$$

with k_{s1} and k_{s2} the solubility equilibrium constants (calculated at 60 °C using the Hess's law). The apparent presence of Zn (near the CdS-ZnO interface) and of Se/Sn/Zn/Cu (close to the CZTSe-CdS interface) into the CdS layer could come from the roughness of the layers and/or from local diffusions. According to the EDX maps acquired on this area,[20] the presence of the "shoulder" visible on Cd and S signals could be due to an inclusion of CdS (~15 nm thickness) in the ZnO layer, supporting the first hypothesis. In any case, no preferential inter-diffusion effect was observed in these regions. When the Mo-CZTSe interface is concerned, we observe a $MoSe_x$ layer (~80 nm) as well as a Cu_xSe layer (~80 nm) between the absorber and the back contact. This Cu segregation at the Mo/CZTSe interface could either be caused by the sample preparation procedure, as shown by Wätjen *et al.*,[22] or due to the reported instability of this interface.[23]

To further analyze the composition of this sample on a larger scale (100 × 100 μm^2), the elemental profile in our devices was determined by SIMS measurement and is shown in Figure 5. The profile of the primary elemental constituents of the absorber (i.e., Cu, Sn, Zn, and Se) is represented in solid lines. The raw SIMS response shows a nominally uniform composition in Cu, Zn, Sn, and Se as a function of depth in the absorber layer. From the comparative analysis of the distribution of these elements, we observe that the Sn content seems slightly lower near the Mo back contact: this could be explained by the presence of the ZnSe and Cu_xSe secondary phases. The Zn profile appears continuous at the front interface (i.e., from ZnO to CZTSe), due to the roughness of the sample. The voids at the interface between the absorber and the back contact can easily explain the apparent blurred transition from CZTSe to Mo. We found a relatively high density of Cd and S atoms within the CZTSe bulk, with V-shape profiles suggesting that both elements are mainly located at the surfaces of the CZTSe grains (i.e., voids at the back contact/absorber interface, top surface). This observation tends to confirm that the amorphous layer containing S and organic matter observed by TEM measurement at the free bottom surface of the absorber is partially formed during the processing of the buffer layer. Although it may appear in contradiction with the previous EDX analysis showing only organic matter on the surface of the bottom CZTSe grains, the sample size analyzed by SIMS is larger than the size of the TEM specimen; therefore, a CdS layer might also be present at this location on some specific areas. We also observed the diffusion into the absorber layer of impurities coming from the SLG substrate, such as Na and K. Both elements show similar diffusion profiles (i.e., higher concentration at the bottom of the absorber

This article is copyrighted as indicated in the article. Reuse of AIP content is subject to the terms at: http://scitation.aip.org/termsconditions. Downloaded to IP: 143.129.150.67 On: Fri, 07 Nov 2014 16:31:50

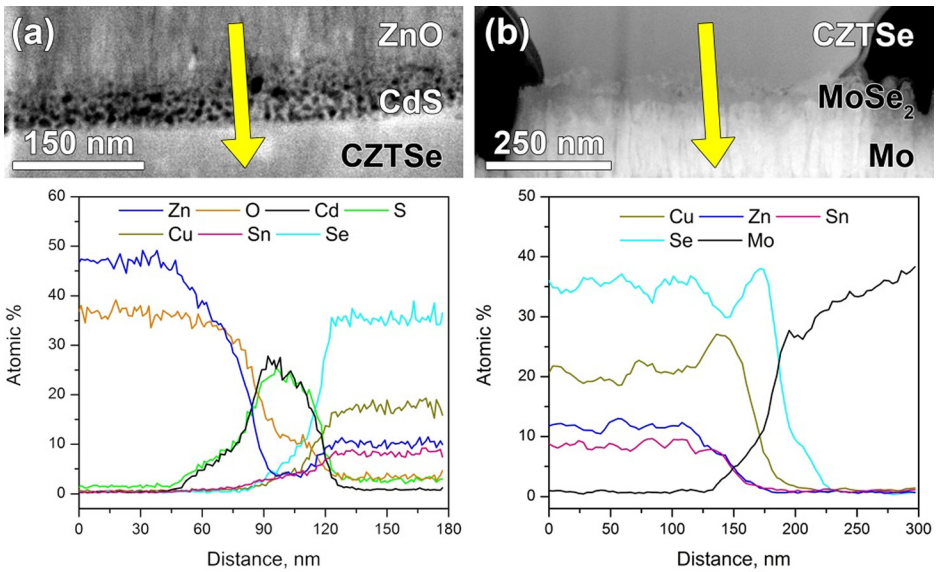

FIG. 4. HAADF-STEM images of the interfaces between absorber/buffer layer (a) and between back contact/absorber (b), and the EDX scans measured across the interfaces.

layer). However, the Na atoms are also present at the front interface, while the K atoms are mainly located close to the back interface. Schwarz *et al*. showed that Na impurities are found to be segregated at certain parts of the CZTSe/ZnSe interfaces and could have an effect on the formation and growth of ZnSe domains.[12] We suggest that Na and K could also segregate at the free surface of the CZTSe grains close to the back contact.

In summary, we have performed investigations on the local morphology and composition of a 9.7% total area efficient CZTSe solar cells. We have observed that the composition of the CZTSe crystallites is quite homogeneous with average values of $Cu_{1.94}Zn_{1.12}Sn_{0.95}Se_{3.99}$. Large crystals of ZnSe-based secondary phase (up to 400 nm diameter) were found at the voids between the absorber and the back contact, while smaller ZnSe domains are segregated at the grain boundaries and close to the surface of the CZTSe grains. The structure of the local point back contact is formed of a stack of Mo-$MoSe_x$-Cu_xSe-CZTSe layers, and the front CZTSe-CdS-ZnO interface seems well defined. The free bottom surface of the absorber at the location of the voids is covered by an amorphous layer containing mainly Cu, S, O, and C, and likely some Cd, Na and K, coming from the chemical bath process and diffusion of species from soda lime glass substrates. As this solar cell shows relatively high efficiency, we conclude that all these particular features are not harmful for the device performances, if not enhancing the electrical properties of the CZTSe absorber.

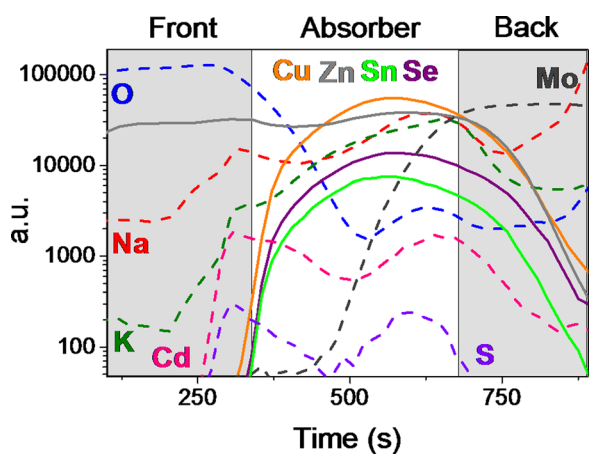

FIG. 5. SIMS elemental profile of the CZTSe-CdS-ZnO solar cell, plotted on a logarithm scale as function of the sputter-etch time. The following elements are represented: Cu, Zn, Sn, Se (in solid lines) and Cd, S, O, Mo, Na, K (in dashed line).

This research was partially funded by the Flemish government, Department Economy, Science and Innovation. We would like to acknowledge Tom De Geyter, Greetje Godiers, and Guido Huyberechts from Flamac in Gent for sputtering of the metal layers. AGC is acknowledged for providing SLG/Mo substrates.

[1]S. Siebentritt and S. Schorr, Prog. Photovoltaics: Res. Appl. **20**, 512 (2012).
[2]S. Delbos, EPJ Photovoltaics **3**, 35004 (2012).
[3]K. Ito and T. Nakazawa, Jpn. J. Appl. Phys., Part 1 **27**, 2094 (1988).
[4]C. Platzer-Björkman, J. Scragg, H. Flammersberger, T. Kubart, and M. Edoff, Sol. Energy Mater. Sol. Cells **98**, 110 (2012).
[5]C. Persson, J. Appl. Phys. **107**, 53710 (2010).
[6]T. Todorov, J. Tang, S. Bag, O. Gunawan, T. Gokmen, Y. Zhu, and D. B. Mitzi, Adv. Energy Mater. **3**, 34 (2013).
[7]W. Wang, M. Winkler, O. Gunawan, T. Gokmen, T. Todorov, Y. Zhu, and D. Mitzi, Adv. Energy Mater. **4**, 1 (2014).
[8]A. Fairbrother, X. Fontané, V. Izquierdo-Roca, M. Placidi, D. Sylla, M. Espindola-Rodriguez, S. López-Mariño, F. Pulgarín, O. Vigil-Galán, A. Pérez-Rodríguez, and E. Saucedo, Prog. Photovoltaics: Res. Appl. **22**, 479–487 (2014).
[9]A. Redinger, K. Hönes, X. Fontané, V. Izquierdo-Roca, E. Saucedo, N. Valle, A. Pérez-Rodríguez, and S. Siebentritt, Appl. Phys. Lett. **98**, 101907 (2011).
[10]T. Tanaka, T. Sueishi, K. Saito, Q. Guo, M. Nishio, K. Yu, and W. Walukiewicz, J. Appl. Phys. **111**, 053522 (2012).
[11]J. Just, D. Lutzenkirchen-Hecht, R. Frahm, S. Schorr, and T. Unold, Appl. Phys. Lett. **99**, 262105 (2011).
[12]T. Schwarz, O. Cojocaru-Miredin, P. Choi, M. Mousel, A. Redinger, S. Siebentritt, and D. Raabe, Appl. Phys. Lett. **102**, 042101 (2013).
[13]S. López-Marino, M. Placidi, A. Pérez-Tomás, J. Llobet, V. Izquierdo-Roca, X. Fontané, A. Fairbrother, M. Espíndola-Rodríguez, D. Sylla, A. Pérez-Rodríguez, and E. Saucedo, J. Mater. Chem. A **1**, 8338 (2013).
[14]J. Scragg, J. Wätjen, M. Edoff, T. Ericson, T. Kubart, and C. Platzer-Björkman, J. Am. Chem. Soc. **134**(47), 19330 (2012).
[15]G. Brammertz, M. Buffière, S. Oueslati, H. ElAnzeery, K. Ben Messaoud, S. Sahayaraj, C. Köble, M. Meuris, and J. Poortmans, Appl. Phys. Lett. **103**, 163904 (2013).

This article is copyrighted as indicated in the article. Reuse of AIP content is subject to the terms at: http://scitation.aip.org/termsconditions. Downloaded to IP: 143.129.150.67 On: Fri, 07 Nov 2014 16:31:50

[16]J. Klaer, I. Luck, A. Boden, R. Klenk, I. Gavilanes Perez, and R. Scheer, Thin Solid Films **431–432**, 534 (2003).
[17]Ch. Köble, D. Greiner, J. Klaer, R. Klenk, A. Meeder, and F. Ruske, Thin Solid Films **518**, 1204 (2009).
[18]M. Buffière, H. ElAnzeery, S. Oueslati, K. Ben Messaoud, G. Brammertz, M. Meuris, and J. Poortmans, "Physical characterization of $Cu_2ZnGeSe_4$ thin films from annealing of Cu-Zn-Ge precursor layers," Thin Solid Films (published online).
[19]B. Mendis, M. Goodman, J. Major, A. Taylor, K. Durose, and D. Halliday, J. Appl. Phys. **112**, 124508 (2012).
[20]See supplementary material at http://dx.doi.org/10.1063/1.4901401 for more HAADF-STEM images, overview EDX maps, and EDX spectra performed on this sample.
[21]G. Brammertz, M. Buffière, Y. Mevel, Y. Ren, A. E. Zaghi, N. Lenaers, Y. Mols, C. Koeble, J. Vleugels, M. Meuris, and J. Poortmans, Appl. Phys. Lett. **102**, 013902 (2013).
[22]J. T. Wätjen, J. J. Scragg, M. Edoff, S. Rubino, and C. Platzer-Björkman, Appl. Phys. Lett. **102**, 051902 (2013).
[23]J. T. Wätjen, J. J. Scragg, T. Ericson, M. Edoff, and C. Platzer-Björkman, Thin Solid Films **535**, 31 (2013).

This article is copyrighted as indicated in the article. Reuse of AIP content is subject to the terms at: http://scitation.aip.org/termsconditions. Downloaded to IP: 143.129.150.67 On: Fri, 07 Nov 2014 16:31:50